EUKARYOTIC CELL, Dec. 2003, p. 1253–1265 Vol. 2, No. 6
1535-9778/03/$08.00+0 DOI: 10.1128/EC.2.6.1253–1265.2003

Use of cDNA Microarrays To Monitor Transcriptional Responses of the Chestnut Blight Fungus *Cryphonectria parasitica* to Infection by Virulence-Attenuating Hypoviruses

Todd D. Allen, Angus L. Dawe, and Donald L. Nuss*

Center for Biosystems Research, University of Maryland Biotechnology Institute, College Park, Maryland 20742-4450

Received 18 June 2003/Accepted 22 August 2003

Hypoviruses are a family of cytoplasmically replicating RNA viruses of the chestnut blight fungus *Cryphonectria parasitica*. Members of this mycovirus family persistently alter virulence (hypovirulence) and related fungal developmental processes, including asexual and sexual sporulation. In order to gain a better understanding of the molecular basis for these changes, we have developed a *C. parasitica* cDNA microarray to monitor global transcriptional responses to hypovirus infection. In this report, a spotted DNA microarray representing approximately 2,200 *C. parasitica* genes was used to monitor changes in the transcriptional profile after infection by the prototypic hypovirus CHV1-EP713. Altered transcript abundance was identified for 295 clones (13.4% of the 2,200 unique cDNAs) as a result of CHV1-EP713 infection—132 up-regulated and 163 down-regulated. In comparison, less than 20 specific *C. parasitica* genes were previously identified by Northern analysis and mRNA differential display as being responsive to hypovirus infection. A 93% validation rate was achieved between real-time reverse transcription-PCR results and microarray predictions. Differentially expressed genes represented a broad spectrum of biological functions, including stress responses, carbon metabolism, and transcriptional regulation. These findings are consistent with the view that infection by a 12.7-kbp hypovirus RNA results in a persistent reprogramming of a significant portion of the *C. parasitica* transcriptome. The potential impact of microarray studies on current and future efforts to establish links between hypovirus-mediated changes in cellular gene expression and phenotypes is discussed.

Viruses are widely distributed throughout the kingdom *Fungi* (2). Members of the mycovirus family *Hypoviridae* are distinguished by the ability to persistently attenuate virulence (hypovirulence) and stably alter dependent developmental processes, e.g., asexual and sexual sporulation, of their host, the chestnut blight fungus *Cryphonectria parasitica* (13). They are also the first viruses of filamentous fungi for which a reverse genetics system was developed, providing the capability to manipulate the genomes of both a eukaryotic virus and its host. Consequently, hypoviruses are unique experimental tools for gaining deeper insights into virus-host interactions and revealing fundamental processes underlying fungal pathogenesis.

The pleiotropic nature of hypovirus-mediated phenotypic changes suggested the perturbation of one or more key regulatory pathways (13). Subsequent studies implicated two principal signal transduction pathways in the manifestation of hypovirus-induced phenotypic changes: G-protein-linked, cyclic AMP (cAMP)-mediated (5, 7, 20, 37) and calcium/calmodulin/inositol trisphosphate-dependent (31, 32) signaling cascades. However, evidence for hypovirus-mediated alteration of these pathways has relied predominantly on single-gene analyses to monitor pathway activity, e.g., the 13-1 gene for G-protein-linked, cAMP-mediated signaling and the *lac-1* (laccase) gene for calcium/calmodulin/inositol trisphosphate-dependent signal transduction. Using differential mRNA display, Chen et al. (5) reported that more than 400 PCR products either increased ($n = 296$) or decreased ($n = 127$) in abundance as a result of infection by the prototypic hypovirus CHV1-EP713. Moreover, similar changes in the accumulation of approximately 65% of these PCR products were observed when G-protein/cAMP signaling was altered in the absence of hypovirus infection. Kang et al. (25) subsequently used the more sensitive ordered differential display approach to estimate that 20% of the total *C. parasitica* genes were modulated following hypovirus CHV1 infection. While mRNA differential display can provide a good indication of the relative extent to which transcriptional profiles change, considerable additional effort is required to determine the identities of differentially expressed genes. We now report the successful use of a spotted expressed sequence tag (EST) array derived from a *C. parasitica* EST (CEST) library consisting of over 4,200 sequences representing approximately 2,200 unique genes (12) to monitor hypovirus-mediated global changes in host gene expression.

MATERIALS AND METHODS

Strains and media. Hypovirus-free *C. parasitica* strain EP155 (ATCC 38755) and isogenic strain EP155/CHV1-EP713 (ATCC 52571), which is infected with the prototypic hypovirus CHV1-EP713 (45), were maintained on potato dextrose agar (PDA; Difco, Detroit, Mich.) at 22 to 24°C with a 12-h light-dark cycle at 1,300 to 1,600 lx. Cultures used for RNA preparations were grown under similar conditions on cellophane membranes overlaying PDA (PDA-cellophane).

Total RNA isolation. Cultures used for RNA isolation were grown on PDA-cellophane for 6 days and harvested by freezing the mycelia in liquid nitrogen and then immediately grinding the mycelia into a fine powder by using a mortar and pestle. The powder was resuspended in RNA extraction buffer (200 mM NaCl, 100 mM Tris-Cl [pH 8.0], 4 mM EDTA [pH 8.0], 2% sodium dodecyl sulfate [SDS], 2 mM dithiothreitol) at a ratio of 4 ml of buffer per g of mycelia. This step was followed sequentially by extraction with equal volumes of water-

* Corresponding author. Mailing address: Center for Biosystems Research, University of Maryland Biotechnology Institute, Plant Sciences Building, Room 5115, College Park, MD 20742-4450. Phone: (301) 405-0334. Fax: (301) 314-9075. E-mail: nuss@umbi.umd.edu.

saturated phenol, acid phenol-chloroform-isoamyl alcohol (125:24:1) (pH 4.5), and chloroform. Single-stranded RNA was precipitated on ice for 2 h by the addition of LiCl to a final concentration of 2 M. The single-stranded RNA precipitate was collected by centrifugation, resuspended in 2 ml of double-distilled H_2O, reprecipitated by the addition of 2.5 volumes of ice-cold ethanol and 0.1 volume of 3 M sodium acetate (pH 5.2), and incubated for 30 min at −20°C. The RNA was collected by centrifugation, washed with 2 ml of ice-cold 75% ethanol, dried, and treated with 2 U of RQ1 DNase (Promega) in 0.5 ml of 20 mM Tris (pH 8.0)–20 mM $MgCl_2$ in the presence of 40 U of RNasin (Promega) for 1 h at 37°C. Following phenol-chloroform and chloroform extractions, the RNA was precipitated with ethanol and resuspended in 100 μl of double-distilled H_2O.

Microarray slide printing. An ordered CEST library was constructed from cDNA prepared from a mixed mRNA population isolated from hypovirus CHV1-EP713-infected *C. parasitica* strain EP155 and uninfected *C. parasitica* strain EP155 cloned into the λZipLox vector (Invitrogen) (12). A large majority (95.7%) of the inserts were sized at 500 to 2,000 bp, and sequencing of 4,216 clones from the 5′ end yielded an average read length of 608 bp (12). A subset of this CEST library was selected for microarray printing by removal of ESTs corresponding to the hypovirus genome and to the highly abundant hydrophobin gene cryparin. The resulting 3,864 ESTs, representing approximately 2,200 unique genes, were reordered to form the array EST (AEST) library used for printing. The accuracy of library reordering was ensured by sequencing eight AEST clones from each 96-well plate used to organize the library. Correspondence between CEST and AEST library clone designations can be accessed at http://www.umbi.umd.edu/~cbr/aesttocest.pdf. PCR fragments used for printing the microarray chip were amplified from the AEST library by using Sp6 and T7 primer sites flanking the inserts in standard 100-μl PCR mixtures. PCR products were analyzed on gels to confirm the success of the reactions and were subsequently purified by using MultiScreen-PCR plates (Millipore). Purified PCR products were resuspended in 50 μl of 3×SSC (1×SSC is 0.15 M sodium chloride plus 0.015 M sodium citrate [pH 7.0]) for printing. Microarray printing and hybridization were performed at the University of Maryland Biotechnology Institute Center for Biosystems Research DNA Microarray Core Facility, which is equipped with an Affymetrix 417 Arrayer and 418 Scanner (http://www.umbi.umd.edu/~cab/microarraymain.html). Purified PCR products were arrayed in duplicate on poly-L-lysine-coated glass slides with an average spot diameter of 100 μm and a spot spacing of 300 μm.

Following printing, the spotted cDNA was cross-linked to the surface of the slides (at 65 mJ) by using a StrataLinker instrument and washed with a 1% SDS solution to minimize the background. Slides were subsequently placed in a blocking solution containing 0.2 M succinic anhydride and 0.05 M sodium borate prepared in 1-methyl-2-pyrrolidinone for 20 min, washed for 2 min in 95°C water, and rinsed five times in 95% ethanol. Slides were spin dried at 500 rpm for 5 min and stored for future hybridizations.

Fluorescent probe generation for hybridization. Fluorescence-labeled cDNA probes were prepared from total RNA purified from uninfected or CHV1-EP713-infected *C. parasitica* strain EP155 (60 μg per probe) by direct incorporation of Cy3- or Cy5-labeled dUTP with Superscript II reverse transcriptase (Invitrogen) and 2 μg of oligo(dT) primer according to the manufacturer's instructions. Unincorporated nucleotides were removed by using a Microcon-30 spin column, and the purified probes were combined for further processing immediately prior to hybridization.

Microarray hybridization and scanning. Printed slides were prepared for hybridization by the addition of 30 μl of prehybridization solution, which contained 50% formamide, 6× SSPE (1× SSPE is 0.15 M NaCl, 0.01 M NaH_2PO_4, and 0.001 M EDTA), 0.5% SDS, 5× Denhardt's solution, and 100 μg of salmon sperm DNA/ml, to the arrayed surface of a glass slide (covered with a coverslip to evenly distribute the prehybridization solution). The slide was incubated for 30 min at 42°C in a hybridization chamber. Fluorescence-labeled probes were dried and resuspended in 20 μl of hybridization solution, which contained 50% formamide, 6× SSPE, 0.5% SDS, 5× Denhardt's solution, blocking solution [2 μg of poly(dA), 4 μg of yeast tRNA, 10 μg of salmon sperm DNA)], 14 μl of master mix solution (70% formamide, 3× Denhardt's solution, 0.7% SDS), and 6 μl of 20× SSPE. The resuspended probes were heated to 100°C for 2 min, vortexed, and collected by a brief spin in a microcentrifuge. The probes were applied to the arrayed surface, covered with a coverslip, and placed in a hybridization chamber overnight at 42°C. Hybridized slides were washed in each of three solutions (solution 1 is 1× SSC– 0.1% SDS, solution 2 is 2× SSC– 0.1% SDS, and solution 3 is 2× SSC) for 10 min, spun dry, scanned in both Cy3 and Cy5 channels with an Affymetrix 418 Scanner at a 10-μm resolution and a 70% photomultiplier tube value, and exported as 16-bit TIFF images for analysis.

Microarray data processing and analysis. Integrated pixel intensity values for each spot were calculated by using TIGR Spotfinder software and saved in tab-delimited format for use by TIGR MIDAS software (The Institure for Genomic Research [TIGR], Rockville, Md.; http://www.tigr.org/software). All hybridization data from three sets of dye-swap experiments were normalized simultaneously in MIDAS to correct for experimental error within a specific hybridization and between repeated hybridizations. With the data processing functions present within MIDAS, intraslide normalization was achieved by applying a locally weighted linear regression (LOWESS) algorithm (smoothing factor, 0.33) on the log ratio-log product plot of the data set for each hybridization (on a block-by-block basis) and adjusting the Cy5 signal for each clone by its calculated LOWESS factor. Interslide normalization was achieved by rescaling the Cy3 and Cy5 signals for each spot on a chip by using the standard deviation of Cy3 and Cy5 signals measured across all hybridizations.

Selection of differentially expressed clones in each hybridization was performed by importing the normalized (and rescaled) Cy3 and Cy5 values calculated in MIDAS into the Functional Genomics module of Spotfire DecisionSite 7.0 (Spotfire, Inc., Somerville, Mass.; www.spotfire.com). The $\log_2$ (Cy3/Cy5) ratio for each clone was calculated, and the clones were divided into groups based on the number of standard deviations by which a specific clone $\log_2$ ratio varied from the data set average $\log_2$ ratio. Clones with $\log_2$ ratios equal to or greater than ±2 standard deviations in a minimum of four of six hybridizations were considered differentially expressed. Genes identified as differentially expressed were hierarchically clustered in Spotfire DecisionSite 7.0.

Validation of differentially expressed clones through real-time RT-PCR. Twenty-eight clones predicted to be differentially expressed by microarray analysis were tested by quantitative reverse transcription (RT)-PCR with an Applied Biosystems (Foster City, Calif.) GeneAmp 5700 sequence detection system and an Applied Biosystems TaqMan RT kit. A single cycle consisting of 10 min at 25°C, 40 min at 48°C, and 5 min at 95°C was used to reverse transcribe 100 ng of RQ1-treated RNA in a 100-μl reaction mixture containing 10 mM Tris-Cl (pH 8.3), 50 mM KCl, 5.5 mM $MgCl_2$, 500 μM each deoxynucleoside triphosphate, 2.5 μM random hexamer, 0.4 U of RNase inhibitor, and 1.25 U of Multiscribe reverse transcriptase/ml. The transcript abundance of each clone of interest was then measured by using quantitative PCR with TaqMan master mix reagents. For each real-time PCR, 2.5 μl of cDNA was incubated with 1 μM each forward and reverse primers and 200 nM probe. For each template measured, 18S rRNA (1:1,000 dilution of cDNA) was measured for normalization. Transcript abundance relative to the amount of 18S rRNA in the sample was calculated by using the comparative threshold cycle method (23) with the primers and conditions described by Parsley et al. (37).

RESULTS

Microarray design and data analysis. The CEST library used in this study was prepared from RNAs isolated from both virus-free *C. parasitica* and hypovirus CHV1-EP713-infected *C. parasitica* to increase the representation of expressed fungal genes (12). Based on BLAST analysis and classifications according to Gene Ontology Consortium (www.geneontology.org) guidelines, the collection was generally representative of the entire population of expressed genes (12). Reordering of the library for microarray printing (AEST library) provided the opportunity to verify clone identity as well as remove certain highly redundant sequences and clones that yielded little or no sequence information. In this manner, the 3,864 spotted cDNAs still represented each of the predicted 2,200 gene products, or between 20 and 25% of the total gene coding potential of *C. parasitica* (12).

Additional elements were incorporated into the design of the CEST spotted array to enhance confidence in the microarray results. A number of control cDNAs were spotted on the microarray to guide data analysis software selection. These included CHV1-EP713 coding regions for p29, p48, and several EST clones representing different portions of open reading frame B that would be expected to increase in signal in-

tensity when hybridized with a CHV1-EP713-specific probe and a *C. parasitica* gene, 13-1, that was recently shown to be CHV1-EP713 inducible (37). Clones containing cDNAs corresponding to ribosomal proteins L8, L3, L15, S10, S27, S8, S25, and S6 and 18S rRNA were included to represent genes not expected to be altered in expression upon hypovirus infection. Clones with no predicted sequence homology to the *C. parasitica* genome were included to monitor signal background levels; these included *Escherichia coli* proteins NusA, LacI, AraC, and RecJ. In addition, each of the 3,864 EST clones was spotted in duplicate. Finally, real-time RT-PCR was used to verify differential transcript accumulation for a subset of genes predicted by microarray analysis to be differentially expressed.

Previous differential mRNA display studies (5, 25) suggested the potential for large differences in specific mRNA levels upon virus infection. To avoid data processing problems associated with cDNA spots that may not have been detectable in one channel due to complete gene repression in the presence or absence of hypovirus, we used the MIDAS software package from TIGR (http://www.tigr.org/software). This software uses a LOWESS algorithm to separate a fluorescent signal of biological significance from noise that is characteristic of microarray studies (40). This package identified all control spots in at least five of the six hybridization replicates performed in this study (Table 1) while avoiding the selection of clones with aberrant signals. mRNA quality was also monitored by spotting all four exons of the *C. parasitica* endothiapepsin (*epn-1*) gene. These exons showed similar magnitudes of a decrease in transcript abundance following hypovirus infection in at least four of six hybridizations (data not shown), suggesting minimal levels of RNA degradation.

Hypovirus CHV1-EP713-mediated modulation of *C. parasitica* transcript accumulation. Figure 1 displays scatter plots for data obtained from four complete hybridizations of the *C. parasitica* microarray chip with two independent RNA preparations. Hybridization 1 was performed with probes specific for RNA isolated from uninfected strain EP155 labeled with Cy3-dUTP and for RNA isolated from CHV1-EP713-infected strain EP155 (EP155/CHV1-EP713) labeled with Cy5-dUTP. Hybridization 1R (where R means reciprocal) was performed with probes made against the same RNA preparations but labeled with the opposite dye: the EP155/CHV1-EP713 probe was labeled with Cy3-dUTP, and the EP155 probe was labeled with Cy5-dUTP. Reciprocal hybridizations 2 and 2R were performed similarly but with an independent set of RNA preparations as a template for probe synthesis. All four hybridizations displayed a tightly packed profile of normalized signal intensity ratios, suggesting that the two independent RNA preparations used for these hybridizations were of similar quality (note the common dynamic range of each hybridization along the *x* and *y* axes). The level of experimental variation between hybridizations is illustrated for a positive control hypovirus sequence, p48 (shaded red triangles), and a down-regulated EST clone, AEST-05-C-02 (shaded green circles). The magnitude of differential expression for these two genes was confirmed by real-time RT-PCR (p48 data not shown; AEST-05-C-02 data shown in Table 2). While minor fluctuations in magnitude were observed for p48 and AEST-05-C-02 measurements, the relative positions within each data set for the two genes were largely consistent between hybridizations.

Figure 2 shows a hierarchical clustering of genes that were scored as differentially expressed and demonstrates the variation between gene measurements across the three reciprocal (six total) hybridizations performed. The intensity of red or green blocks in Fig. 2 is reflective of $\log_2$ (Cy3/Cy5) measurements for each gene across hybridizations. Because of missing data (gray blocks), attributable to hybridization anomalies, or low log ratios (black blocks) for some genes, we chose to designate a gene as differentially expressed if the corresponding log ratio was at least 2 standard deviations from the experimental average log ratio for a minimum of four of the six hybridizations performed. On the basis of this criterion, a total of 295 EST clones, 13.4% of the 2,200 unique genes represented on the microarrray, were scored as being responsive to CHV1-EP713 infection. The accumulation of transcripts for 132 genes was observed to increase after hypovirus infection, while decreases in transcript accumulation were observed for 163 genes.

In an effort to gain insight into the biological significance of the CHV1-EP713-mediated change in the host transcriptional profile, the differentially expressed ESTs were related to putative biological processes assigned by Dawe et al. (12) according to classification guidelines outlined by the Gene Ontology Consortium (www.geneontology.org). Since a number of genes on the microarray chip were represented by multiple EST clones (12), the list of differentially expressed clones was initially filtered to ensure that GenBank identification numbers were present only once. Nevertheless, the list still retained a small number of clones (less than 10% of the list) with distinct GenBank identification numbers that were identified as the same protein in different organisms (for example, AEST-03-E-12 and AEST-13-A-03 are cytochrome P450 monooygenases from *Penicillium paxilli* and *Neurospora crassa*, respectively). Assignments by Dawe et al. (12) were limited to genes with BLAST *E* values of 10^{-10} or less, corresponding to 162 of the 295 differentially expressed genes. As indicated in Table 1, 118 hypovirus-responsive genes were broadly distributed throughout the available biological process categories, consistent with the pleiotrophic nature of CHV1-EP713-mediated phenotypic changes. An additional 44 showed significant matches with genes of unknown function.

Microarray versus real-time RT-PCR analysis. Although several features had been built into the microarray design to enhance confidence in the microarray results, it was important to validate the differential expression values by independent means. Real-time RT-PCR was adopted because of its high level of sensitivity, its potential speed of validation, and the requirement for low quantities of test material compared to those needed for Northern analysis (3).

A subset of 28 genes predicted by microarray analysis to be differentially expressed was chosen for confirmation based on putative function or magnitude of differential transcript accumulation. Each clone tested by kinetic RT-PCR was measured in triplicate for each of two independent RNA isolations (Table 2). A total of 26 out of 28 clones were confirmed by real-time RT-PCR analysis, indicating a 93% success rate for accurately identifying differentially expressed clones.

TABLE 1. Genes differentially expressed in EP155 and EP155/CHV1-EP713[a]

AEST	Expression in CHV1-EP713[b]	Avg fold change[c]	Description[d]
Microarray controls			
p48	Up	64.08	Hypovirus encoded
p29	Up	62.29	Hypovirus encoded
Open reading frame B	Up	14.47	Hypovirus encoded
13-1	Up	5.04	*C. parasitica* encoded
epn-1 (exon 1)	Down	3.40	*C. parasitica* encoded (endothiapepsin)
epn-1 (exon 2)	Down	4.18	*C. parasitica* encoded (endothiapepsin)
epn-1 (exon 3)	Down	3.69	*C. parasitica* encoded (endothiapepsin)
epn-1 (exon 4)	Down	3.02	*C. parasitica* encoded (endothiapepsin)
Amino acid metabolism			
AEST-07-D-03	Down	2.52	Conserved hypothetical protein (*Neurospora crassa*) Arginase family protein (*Schizosaccharomyces pombe*)
AEST-08-F-10[e]	Up	23.69	SAMS (*Neurospora crassa*)
AEST-16-C-03	Down	3.59	Dialkylglycine decarboxylase (*Burkholderia cepacia*)
AEST-22-H-07	Down	4.95	Putative tyrosinase (*Gibberella zeae*)
AEST-24-D-03	Down	2.97	Putative 1,2-dioxygenase (*Escherichia coli*)
AEST-28-G-11	Up	3.58	Hypothetical protein (*Neurospora crassa*) Lysine biosynthesis, oxidative stress protection; Lys7p (*Saccharomyces cerevisiae*)
AEST-31-E-07	Up	2.16	Methionine adenosyltransferase (*Neurospora crassa*)
Cell cycle			
AEST-07-B-12[e]	Up	4.72	GTP-binding nuclear protein SPI1 (*Neurospora crassa*)
AEST-10-A-11[e]	Down	2.99	Probable cell division control protein 10 (*Neurospora crassa*)
AEST-25-H-08	Down	3.69	Hypothetical protein (*Neurospora crassa*) GTP-binding protein homologue (*Lawsonia intracellularis*)
AEST-26-C-03	Down	2.67	U83489 septin B (*Aspergillus nidulans*)
Carbohydrate metabolism			
AEST-08-F-03	Down	2.52	Hypothetical protein (*Neurospora crassa*) Phosphoglucomutase (*Aspergillus oryzae*)
AEST-11-A-04[e]	Down	4.09	Hypothetical protein (*Neurospora crassa*) Probable glucose transporter RCO-3 (*Neurospora crassa*)
AEST-11-B-09	Down	2.64	Hypothetical protein (*Neurospora crassa*) α-Mannosidase Class 1 (*Emericella nidulans*)
AEST-11-E-12	Down	2.67	D-Xylose reductases II and III (*Candida tropicalis*)
AEST-11-F-11	Down	4.15	Chain A, α1,2-mannosidase (*Trichoderma reesei*)
AEST-12-F-01	Down	3.30	Probable transketolase (*Neurospora crassa*)
AEST-15-A-05	Down	2.31	Conserved hypothetical protein (*Corynebacterium efficiens* YS-314) Nucleoside diphosphate sugar epimerases (*Corynebacterium efficiens*)
AEST-16-D-06	Down	2.45	Hypothetical protein (*Neurospora crassa*) Glucosamine-6-phosphate isomerase (*Bacteroides thetaiotaomicron*)
AEST-19-G-03	Down	3.43	Hypothetical protein (*Neurospora crassa*) Mannosyl-oligosaccharide α-1,2-mannosidase (*Aspergillus phoenicis*)
AEST-22-B-11	Up	3.42	Hypothetical protein (*Neurospora crassa*) Putative SAHH (*Saccharomyces cerevisiae*)
AEST-24-A-07	Down	2.99	α-Galactosidase (EC 3.2.1.22) (*Zygosaccharomyces cidri*)
AEST-30-G-01	Down	4.28	Hypothetical protein (*Neurospora crassa*) Acid-stable α-amylase (*Aspergillus kawachii*)
AEST-31-F-10	Down	2.70	Hypothetical protein (*Neurospora crassa*) Probable UTP glucose-1-phosphate uridylyltransferase (*Schizosaccharomyces pombe*)
AEST-31-G-03	Down	3.12	Hypothetical protein (*Neurospora crassa*) Putative membrane protein family member (*Caenorhabditis elegans*)
AEST-35-G-03	Down	2.36	Lactonohydrolase (*Fusarium oxysporum*)
AEST-37-F-03	Down	4.92	β-Glucosidase homologue (*Cochliobolus heterostrophus*)
Cellular recognition			
AEST-09-A-05	Down	2.48	Modin (*Podospora anserina*)
Cell wall growth			
AEST-02-C-10	Up	2.92	3,4-Dihydroxy-2-butanone-4-phosphate synthase (*Magnaporthe grisea*)
AEST-03-D-01	Up	2.34	Hypothetical protein (*Neurospora crassa*) Putative ubiquinone biosynthesis protein (*Schizosaccharomyces pombe*)
AEST-06-B-10	Down	2.33	Hypothetical protein (*Neurospora crassa*) Inositol monophosphatase; Inm1p (*Saccharomyces cerevisiae*)
AEST-12-A-09	Down	2.98	Conserved hypothetical protein (*Neurospora crassa*) Related to spore coat protein SP96 precursor (*Neurospora crassa*)

Continued on following page

TABLE 1—*Continued*

AEST	Expression in CHV1-EP713[b]	Avg fold change[c]	Description[d]
AEST20-G-02	Down	5.53	Predicted protein (*Neurospora crassa*) Hard surface-induced protein 3 (*Glomerella cingulata*)
AEST-22-D-07	Down	2.74	Conserved hypothetical protein (*Neurospora crassa*) Cell wall protein Awa1p (*Saccharomyces cerevisiae*)
AEST-23-A-08	Down	2.80	α-Tubulin (*Colletotrichum lagenarium*)
AEST-23-C-12	Down	2.58	OSJNBa0029H02.25 (*Oryza sativa* cv. Japonica group)
AEST-24-H-11	Down	2.92	Hypothetical protein (*Neurospora crassa*) Putative cell wall biogenesis protein (*Schizosaccharomyces pombe*)
AEST-25-F-06	Down	2.21	Predicted protein (*Neurospora crassa*) Extracellular matrix protein precursor (*Fusarium oxysporum*)
AEST-31-G-11	Up	3.77	Hypothetical protein (*Burkholderia fungorum*) 1-Aminocyclopropane-1-carboxylate oxidase (kidney bean)
AEST-32-A-05	Down	3.65	Hydroxyproline-rich glycoprotein DZ-HRGP (*Volvox carteri* f. sp. *nagariensis*)
AEST-32-H-10	Up	4.07	Related to DFG5 protein (*Neurospora crassa*)
AEST-33-H-04	Down	3.08	Glycine-rich cell wall protein (*Mesorhizobium loti*)
AEST-36-G-02	Up	8.22	Hypothetical protein (*Neurospora crassa*) β-D-Glucoside glucohydrolase (*Hypocrea jecorina*)
Development			
AEST-01-G-04	Up	2.79	Hypothetical protein (*Neurospora crassa*) Apoptosis-regulating basic protein (*Mus musculus*)
AEST-12-D-05	Down	2.53	Putative pheromone response (*Schizosaccharomyces pombe*)
AEST-30-F-01	Down	3.94	Clock-controlled protein 6 (*Neurospora crassa*)
AEST-32-A-06	Down	5.44	Hypothetical protein (*Neurospora crassa*) MAS3 protein (*Magnaporthe grisea*)
AEST-37-G-09	Down	3.66	Hypothetical protein (*Neurospora crassa*) NCP1 (*Cryptococcus neoformans*)
AEST-38-A-06	Down	4.05	Putative protein (*Neurospora crassa*) *Emericella* sexual development C, sexual development (*Aspergillus nidulans*)
Energy pathway			
AEST-34-A-10	Down	3.05	Pyruvate carboxylase (*Aspergillus terreus*)
AEST-38-D-07	Up	2.79	Hypothetical protein (*Neurospora crassa*) Pyruvate dehydrogenase e1 component (*Schizosaccharomyces pombe*)
Electron transport			
AEST-03-E-12	Up	4.52	Cytochrome P450 monooxygenase (*Penicillium paxilli*)
AEST-04-A-11	Up	5.60	Hypothetical protein (*Burkholderia fungorum*) Probable oxidoreductase (*Pseudomonas aeruginosa* PAO1)
AEST-13-A-03[e]	Up	7.95	Cytochrome P450 monooxygenase (*Neurospora crassa*)
AEST-23-B-03	Down	2.92	NAD-dependent formate dehydrogenase (*Mycosphaerella graminicola*)
AEST-24-C-03	Up	3.35	NADH oxidase (*Aspergillus fumigatus*)
AEST-24-D-10	Up	3.09	Hypothetical protein (*Microbulbifer degradans* 2–40) Oxidoreductase (*Clostridium acetobutylicum*)
AEST-24-H-08	Up	3.56	*O*-Methyltransferase (*Aspergillus parasiticus*)
AEST-25-E-05	Up	3.62	Hypothetical protein (*Neurospora crassa*) Oxygenase-like protein (*Streptomyces aureofaciens*)
AEST-26-D-02	Up	3.91	Hypothetical protein (*Neurospora crassa*) Putative oxidoreductase; MmyG [*Streptomyces coelicolor* A3(2)]
AEST-26-G-08	Up	3.71	Hypothetical protein (*Neurospora crassa*) Bifunctional P450:NADPH-P450 reductase (*Fusarium oxysporum*)
AEST-32-C-04	Up	4.18	Probable oxidoreductase (*Pseudomonas aeruginosa* PAO1)
AEST-38-A-11	Up	2.34	Oxidoreductase (*Bacillus halodurans*)
Lipid metabolism			
AEST-03-C-12	Down	2.46	Hypothetical protein (*Neurospora crassa*) Serine palmitoyltransferase 2 (*Schizosaccharomyces pombe*)
AEST-11-C-02	Up	3.69	Hypothetical protein (*Neurospora crassa*) Similar to LTA4 hydrolase (*Homo sapiens*)
AEST-15-F-03	Down	3.18	Probable triacylglycerol lipase precursor (*Neurospora crassa*)
AEST-26-G-05	Down	2.33	Hypothetical protein (*Arabidopsis thaliana*) Phosphatidylglycerol-specific phospholipase C (*Arabidopsis thaliana*)
Metabolism related			
AEST-06-B-03[e]	Down	6.19	Unnamed protein product (*Podospora anserina*) Possible CGI-83 protein (*Leishmania major*)
AEST-13-C-05	Up	6.49	Probable isoamyl alcohol oxidase (*Neurospora crassa*)
AEST-15-D-07	Down	3.26	Probable dehydrogenase (*Mesorhizobium loti*)
AEST-17-D-12	Down	3.22	Acid phosphatase precursor (*Yarrowia lipolytica*)
AEST-18-B-05	Up	2.51	Reductase (*Gibberella zeae*)

Continued on following page

TABLE 1—*Continued*

AEST	Expression in CHV1-EP713[b]	Avg fold change[c]	Description[d]
AEST-19-B-01	Down	3.22	Hypothetical protein (*Neurospora crassa*) Sulfate adenylyltransferase (*Emericella nidulans*)
AEST-20-A-03[e]	Up	18.83	FK506-binding protein 2 precursor (*Neurospora crassa*)
AEST-28-C-01	Up	3.99	Hypothetical protein (*Neurospora crassa*) Putative acetyltransferase (*Clostridium tetani* E88)
AEST-28-D-08	Up	3.11	Hypothetical short-chain dehydrogenase (*Schizosaccharomyces pombe*)
AEST-36-F-03	Down	2.93	Hypothetical protein (*Neurospora crassa*) Aflatoxin B1 aldehyde reductase 1 (*Mus musculus*)
AEST-40-B-12	Down	2.62	Hypothetical protein (*Neurospora crassa*) Protein kinase, putative (*Arabidopsis thaliana*)
Nucleic acid metabolism			
AEST-04-G-09	Down	2.79	CYT-19 DEAD-box protein precursor (*Neurospora crassa*)
AEST-05-C-02[e]	Down	6.20	Hydrogenase regulation; HoxX (*Aquifex aeolicus*)
AEST-05-F-11	Down	4.03	Nuclease PA3 (*Penicillium* sp.)
AEST-06-C-04	Up	2.77	Hypothetical protein (*Neurospora crassa*) Diadenosine tetraphosphatase (*Schizosaccharomyces pombe*)
AEST-08-E-11	Up	11.45	Hypothetical protein (*Neurospora crassa*) ATP synthase β subunit (*Brucella melitensis*)
AEST-11-E-06	Up	3.11	Hypothetical protein (*Neurospora crassa*) Transcriptional regulator (*Clostridium tetani* E88)
AEST-17-E-03	Down	3.14	DNase 1 protein (*Metarhizium anisopliae* var. anisopliae)
AEST-18-D-08	Up	2.31	Probable Snod-Protein 1 precursor (*Neurospora crassa*)
AEST-25-B-11[e]	Down	3.54	Nuclease P1 (*Penicillium citrinum*)
AEST-27-F-10[e]	Down	3.18	Transcriptional regulatory protein Pro1 (*Neurospora crassa*)
AEST-30-C-09[e]	Down	4.95	Mst12 (*Magnaporthe grisea*)
Nuclear organization			
AEST-30-G-04	Up	2.94	Hypothetical protein (*Neurospora crassa*) Sir2-like isoform 5 (*Saccharomyces cerevisiae*)
AEST-37-E-05	Down	2.62	Hypothetical protein (*Neurospora crassa*) DNA-binding protein HEXBP (*Leishmania major*)
Oxygen radical metabolism			
AEST-10-C-08	Up	5.45	Cytochrome P450 (*Coriolus versicolor*)
AEST-11-E-09	Up	4.94	Cytochrome P450 (*Arabidopsis thaliana*)
AEST-31-F-09	Up	8.90	Hypothetical protein (*Neurospora crassa*) Fum12p (*Gibberella moniliformis*)
Protein metabolism			
AEST-05-A-09[e]	Down	4.73	Aspergillopepsin II precursor (*Aspergillus niger*)
AEST-05-E-01[e]	Up	9.86	Probable zinc metalloprotease (*Neurospora crassa*)
AEST-08-C-09	Down	3.19	Acid proteinase EapB precursor (*Cryphonectria parasitica*)
AEST-18-C-11	Down	3.09	Carboxypeptidase S1 (*Penicillium janthinellum*)
AEST-24-H-04[e]	Down	4.08	Endothiapepsin precursor (*Cryphonectria parasitica*)
AEST-26-E-03	Up	2.99	Related to calpain (*Neurospora crassa*)
AEST-28-E-10	Down	2.55	Aspartic protease precursor (*Botryotinia fuckeliana*)
AEST-34-C-05	Down	3.08	Aorsin (*Aspergillus oryzae*)
AEST-36-D-03	Down	2.19	Acid proteinase EapC precursor (*Cryphonectria parasitica*)
AEST-38-C-10	Up	5.51	Ubiquitin-conjugating enzyme E2 (*Magnaporthe grisea*)
Ribosome translation			
AEST-26-F-12	Up	5.46	Hypothetical protein (*Neurospora crassa*) 60S ribosomal protein L10 (*Schizosaccharomyces pombe*)
AEST-39-E-08	Down	2.45	Elongation factor 1-α (*Podospora curvicolla*)
Secondary metabolism			
AEST-14-H-02	Down	3.00	Hypothetical protein (*Neurospora crassa*) Polyketide synthase (*Penicillium citrinum*)
AEST-36-F-02	Up	3.37	Hypothetical protein (*Neurospora crassa*) Probable ketoacyl reductase (*Saccharopolyspora spinosa*)
Stress response			
AEST-02-E-09	Up	2.76	Antifreeze glycoprotein precursor (*Notothenia coriiceps*)
AEST-10-H-10[e]	Up	5.61	Heat shock 70-kDa protein (*Ajellomyces capsulatus*)
AEST-12-G-04[e]	Up	4.85	Hypothetical protein (*Neurospora crassa*) Putative GST (*Schizosaccharomyces pombe*)
AEST-38-C-04	Down	4.00	HSP70 (*Neurospora crassa*)

Continued on following page

TABLE 1—*Continued*

AEST	Expression in CHV1-EP713[b]	Avg fold change[c]	Description[d]
Transport			
AEST-01-F-12	Up	2.43	Hypothetical protein (*Neurospora crassa*) Mitochondrial-import-stimulating-factor transporter (*Schizosaccharomyces pombe*)
AEST-01-G-12[e]	Up	9.31	Hypothetical protein (*Neurospora crassa*) Nontransporter ATP-binding cassette protein AbcF2 (*Dictyostelium discoideum*)
AEST-03-E-10	Up	2.64	Major facilitator superfamily (*Leptosphaeria maculans*)
AEST-22-A-11	Up	3.76	Stomatin-like protein (*Gibberella fujikuroi*)
AEST-27-E-05	Down	3.44	Putative vesicular acetylcholine transporter (*Schizosaccharomyces pombe*)
AEST-34-D-02	Down	2.88	Hypothetical protein (*Neurospora crassa*) Possible membrane drug transporter (*Schizosaccharomyces pombe*)
Unknown			
AEST-01-E-12	Up	3.96	Unnamed protein product (*Podospora anserina*)
AEST-01-G-01	Down	3.73	Predicted protein (*Neurospora crassa*)
AEST-01-H-04	Down	2.52	Predicted protein (*Neurospora crassa*)
AEST-02-D-07	Down	2.41	Predicted protein (*Neurospora crassa*)
AEST-02-E-07	Down	2.60	Hypothetical protein B24B19.80 (*Neurospora crassa*)
AEST-02-F-06	Up	4.55	Hypothetical protein (*Rhodopseudomonas palustris*)
AEST-03-B-06	Down	2.33	Hypothetical protein (*Neurospora crassa*)
AEST-03-F-01	Up	2.24	Hypothetical protein (*Neurospora crassa*) Probable rAspf9 allergen (*Neurospora crassa*)
AEST-06-E-06	Up	2.42	Predicted protein (*Neurospora crassa*)
AEST-07-A-05	Down	3.85	Hypothetical protein (*Neurospora crassa*)
AEST-07-G-09	Down	3.47	Predicted protein (*Neurospora crassa*)
AEST-09-A-11	Down	4.30	Predicted protein (*Neurospora crassa*)
AEST-09-F-04	Down	3.01	Putative protein (*Neurospora crassa*)
AEST-09-F-06	Down	3.24	Hypothetical protein (*Neurospora crassa*)
AEST-12-G-01	Down	2.67	Predicted protein (*Neurospora crassa*)
AEST-13-B-07	Up	2.01	Hypothetical protein (*Neurospora crassa*)
AEST-13-D-06	Down	3.41	Predicted protein (*Neurospora crassa*)
AEST-13-E-03	Up	7.88	Predicted protein (*Neurospora crassa*)
AEST-14-A-06[e]	Up	5.93	Hypothetical protein (*Neurospora crassa*) Trim4 allergen (*Arthroderma benhamiae*)
AEST-14-E-09	Up	6.37	Hypothetical protein (*Neurospora crassa*)
AEST-15-C-06	Down	3.11	Predicted protein (*Neurospora crassa*)
AEST-15-F-01	Down	2.94	Conserved hypothetical protein (*Neurospora crassa*) Trunk lateral cell-specific gene; HrTLC1 (*Halocynthia roretzi*)
AEST-15-F-06	Up	2.38	Predicted protein (*Neurospora crassa*)
AEST-16-C-08	Up	3.27	Hypothetical protein (*Neurospora crassa*)
AEST-16-E-05	Down	2.48	Hypothetical protein (*Neurospora crassa*)
AEST-16-G-02	Down	3.05	Hypothetical protein (*Neurospora crassa*)
AEST-18-H-07	Down	4.62	Hypothetical protein (*Neurospora crassa*)
AEST-19-A-08	Up	5.51	Predicted protein (*Neurospora crassa*)
AEST-21-E-10	Up	4.92	Predicted protein (*Neurospora crassa*)
AEST-22-A-09	Down	8.00	Predicted protein (*Neurospora crassa*)
AEST-22-C-05	Down	3.09	Very large virion protein (tegument) (Bovine herpesvirus 1)
AEST-23-C-03	Down	3.92	Predicted protein (*Neurospora crassa*)
AEST-23-G-11	Up	3.99	Predicted protein (*Neurospora crassa*)
AEST-25-C-02	Down	2.45	CG2839-PA (*Drosophila melanogaster*)
AEST-26-B-03[e]	Up	3.94	Predicted protein (*Neurospora crassa*)
AEST-33-D-08	Up	9.04	Hypothetical protein (*Neurospora crassa*)
AEST-33-E-07	Down	2.52	Predicted protein (*Neurospora crassa*)
AEST-34-B-03	Down	8.39	Hypothetical protein (*Neurospora crassa*)
AEST-34-B-07	Down	2.99	Unnamed protein product (*Podospora anserina*)
AEST-35-D-09	Down	3.01	Predicted protein (*Neurospora crassa*)
AEST-36-A-02	Up	4.70	Predicted protein (*Neurospora crassa*)
AEST-37-D-10	Down	3.35	Predicted protein (*Neurospora crassa*)
AEST-37-F-12	Down	2.84	Epstein-Barr nuclear antigen 1 (Human herpesvirus 4)
AEST-38-E-03	Up	2.52	Hypothetical protein (*Neurospora crassa*)

[a] A total of 162 unique clone identification names were sorted by a previously reported ontology of an EST library (12) based on BLAST *E* values of $\leq 10^{-10}$. The remaining 133 differentially expressed clones had poor BLAST values (*E* values of $> 10^{-10}$) and were not assigned an ontological classification; they are not included here, but can be accessed at http://www.umbi.umd.edu/~cbr/155_713SUPdata.pdf. Clones were assigned to a respective ontology based on the strongest BLAST hit for that clone. In some instances, clones were placed into a group based on secondary BLAST hit (still an *E* value of $\leq 10^{-10}$) when the strongest hit failed to provide an obvious classification. Correspondence between AEST and CEST library clone designations is available at http://www.umbi.umd.edu/~cbr/aesttocest.pdf. The BLAST E value is a measure of the statistical significance of a match with a protein sequence entry present in the database searched by the BLAST algorithm. The lower the E value, the more significant the match.

[b] Increased or decreased mRNA abundance in EP155/CHV1-EP713 relative to EP155.

[c] Average fold change in transcript accumulation for a clone measured across six hybridizations.

[d] Brief biological process description from the strongest BLAST hit for a clone, as well as the corresponding source organism of the matched sequence. When a clone was grouped based on a secondary BLAST hit, the strongest biological process description is listed first, followed by the biological process used to group the clone.

[e] For this clone, a real-time RT-PCR confirmation was performed (see corresponding clone in Table 2).

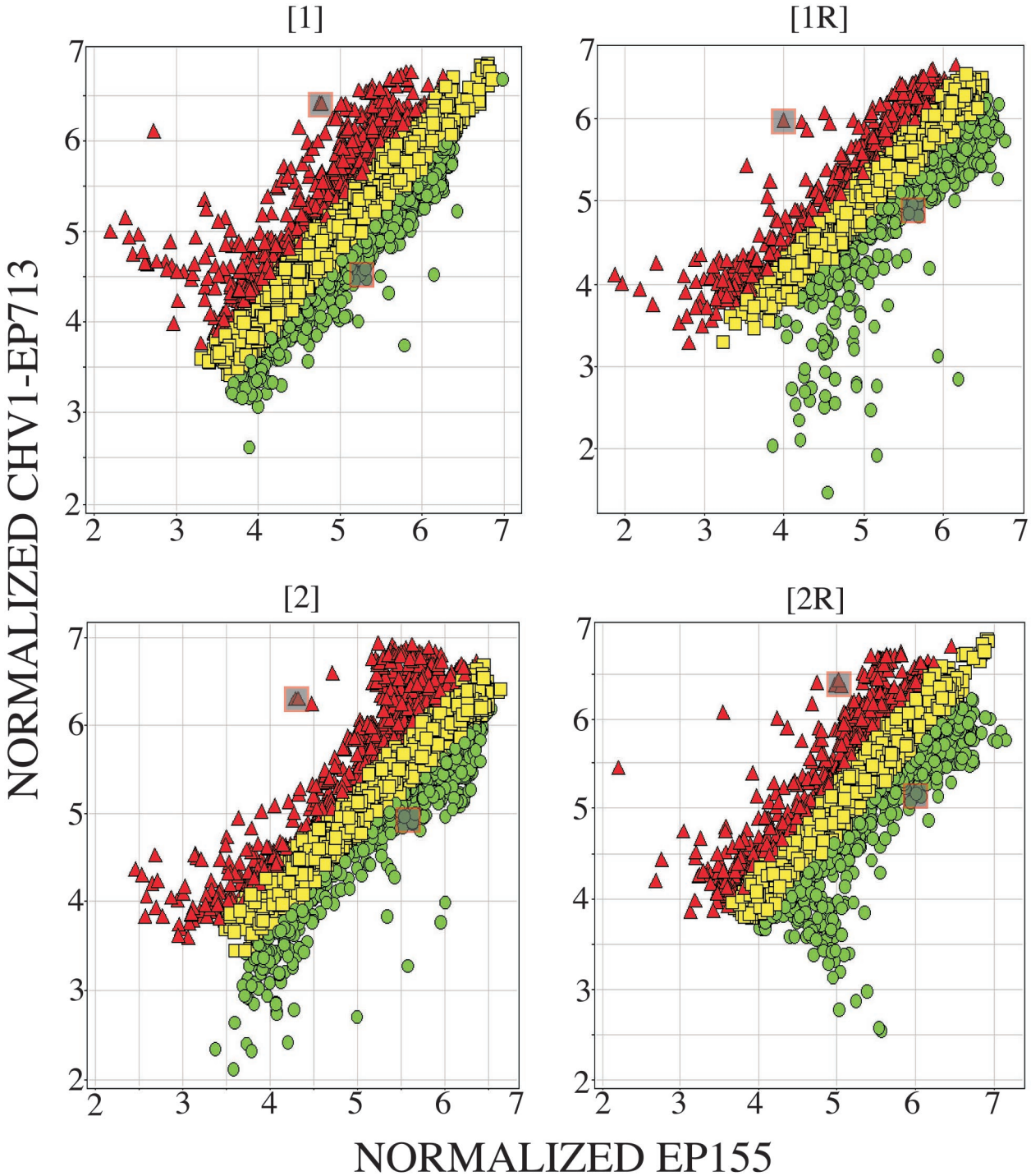

FIG. 1. Scatter plot of four independent hybridizations comparing fluorescence-labeled cDNA probes derived from uninfected strain EP155 and from infected strain EP155/CHV1-EP713. Normalized signals for each channel are plotted on a logarithmic scale. Red triangles represent clones for which transcript accumulation increased in EP155/CHV1-EP713 relative to EP155. Green circles represent clones for which transcript accumulation decreased in EP155/CHV1-EP713 relative to EP155. Clones for which transcript levels did not significantly change after hypovirus infection are represented by yellow squares. Hybridizations 1 and 1R are dye-swap experiments done with the same RNA preparations from EP155 and EP155/CHV1-EP713. Hybridizations 2 and 2R are dye-swap experiments done with samples from a second, independent RNA isolation. Shaded red triangles in each data set indicate the magnitude of differential expression for hypovirus-encoded protein p48. Shaded green circles indicate the magnitude of differential expression for clone AEST-05-C-02.

TABLE 2. Validation of microarray measurements by real-time RT-PCR[a]

Clone	RNA prepn 1		RNA prepn 2		Microarray expt prediction (fold change)
	Ct[b]	Fold change[c]	Ct[b]	Fold change[c]	
AEST-01-G-12	−1.50	2.82 (Up)	−1.19	2.29 (Up)	Up 9.31
AEST-05-E-01	−0.98	1.97 (Up)	−1.36	2.57 (Up)	Up 9.86
AEST-07-B-12	−1.24	2.37 (Up)	−0.92	1.89 (Up)	Up 4.72
AEST-08-F-10	−2.92	7.59 (Up)	−2.69	6.44 (Up)	Up 23.69
AEST-09-H-07 (SUP)	−1.23	2.34 (Up)	−1.12	2.18 (Up)	Up 6.22
AEST-10-H-10	−1.51	2.85 (Up)	−1.42	2.67 (Up)	Up 5.61
AEST-12-G-04	−3.74	13.36 (Up)	−2.66	6.31 (Up)	Up 4.85
AEST-13-A-03	−2.07	4.19 (Up)	−4.21	18.46 (Up)	Up 7.95
AEST-14-A-06[d]	0.57	1.49 (Down)	0.16	1.12 (Down)	Up 5.93
AEST-16-D-11 (SUP)	−3.45	10.95 (Up)	−4.23	18.77 (Up)	Up 4.65
AEST-20-A-03[d]	−0.58	1.49 (Up)	−0.29	1.22 (Up)	Up 18.83
AEST-26-B-03	−3.13	8.75 (Up)	−3.7	13.00 (Up)	Up 3.94
AEST-22-B-11	−1.79	3.46 (Up)	−2.74	6.67 (Up)	Up 3.42
AEST-34-G-04 (SUP)	−5.61	48.84 (Up)	−6.01	64.30 (Up)	Up 9.64
13-1 (positive control)	−4.96	31.16 (Up)	−6.57	94.79 (Up)	Up 5.04
AEST-04-D-04 (SUP)	5.19	36.50 (Down)	5.59	48.17 (Down)	Down 8.98
AEST-05-A-09	3.15	8.88 (Down)	2.35	5.10 (Down)	Down 4.73
AEST-05-C-02	3.88	14.67 (Down)	2.69	6.45 (Down)	Down 6.20
AEST-05-D-11 (SUP)	9.03	522.76 (Down)	10.12	1,112.82 (Down)	Down 6.78
AEST-06-B-03	5.73	53.08 (Down)	7.44	173.65 (Down)	Down 6.19
AEST-09-G-11 (SUP)	4.61	24.42 (Down)	5.33	40.22 (Down)	Down 5.73
AEST-10-A-11	1.19	2.28 (Down)	0.87	1.83 (Down)	Down 2.99
AEST-11-A-04	2.77	6.81 (Down)	2.03	4.08 (Down)	Down 4.09
AEST-24-H-04	1.14	2.21 (Down)	1.76	3.39 (Down)	Down 4.08
AEST-25-B-11	2.89	7.43 (Down)	2.56	5.91 (Down)	Down 3.54
AEST-27-F-10	1.78	3.47 (Down)	1.36	2.57 (Down)	Down 3.18
AEST-30-C-09	1.66	3.16 (Down)	1.25	2.38 (Down)	Down 4.95
AEST-33-F-04 (SUP)	4.73	26.54 (Down)	3.42	10.73 (Down)	Down 6.76

[a] Real-time RT-PCR measurements were obtained for 28 clones predicted to be differentially expressed between EP155 and EP155/CHV1-EP713 by microarray analysis. Measurements were made in triplicate for each clone with two independent total RNA preparations. See Materials and Methods for details. Note that only a subset of the validated clones appears in Table 1, since some (indicated by the abbreviation SUP) are among the 133 clones that had poor BLAST values and that are included in the supplemental data at http://www.umbi.umd.edu/~cbr/155_713SUPdata.pdf.

[b] Average, normalized, and calibrated threshold cycle (Ct) for each clone in each RNA preparation.

[c] Average fold change in hypovirus-infected strain EP155/CHV1-EP713 relative to uninfected strain EP155.

[d] This clone produced inconsistent results between microarray and real-time RT-PCR experiments.

DISCUSSION

One of the remarkable features of hypovirus infection is the ability of a 12.7-kbp genome to stably alter multiple phenotypic traits, ranging from asexual sporulation to virulence. Previous studies with mRNA differential display technologies indicated that these broad phenotypic changes correlated with extensive and persistent alterations in the host transcriptional profile (5). The construction of a *C. parasitica* cDNA microarray now provides many advantages over previous labor-intensive techniques for monitoring transcriptional responses to hypovirus infection. Simultaneous monitoring of the responses of 2,200 unique *C. parasitica* cDNA clones in the present study revealed 295 CHV1-EP713-responsive host genes, corresponding to 13.4% of the unique genes contained on the *C. parasitica* cDNA microarray chip. This value compares well with the estimate of 20% obtained by Kang et al. (25) using an ordered differential display and is not inconsistent with the report by Chen et al. (5) using a conventional mRNA differential display. Assuming that *C. parasitica*, like the closely related fungus *N. crassa* (19), has approximately 10,000 genes within its genome, it is likely that CHV1-EP713 infection results in altered transcript accumulation for approximately 1,300 host genes.

Microarray and real-time RT-PCR results were in excellent agreement with respect to the direction of changes in transcript accumulation, i.e., up-regulated or down-regulated; however, results from the two methods did differ occasionally in the magnitude of changes. This finding was not surprising, given that cross-hybridization between closely related genes can occur on the surface of the microarray slide. Moreover, the fluorescent signal corresponding to a specific mRNA probe can be titrated out due to the presence of redundant copies of the sequence on the microarray slide. Although the accuracy of microarray data can be problematic (40, 51, 53), the 93% validation rate obtained for the *C. parasitica* chip (Table 2) provides a high level of confidence in the list of responsive genes presented in Table 1.

It is noteworthy that the microarray results showed a level of inconsistency with published observations for two previously characterized *C. parasitica* genes—the laccase gene *lac-1* and the gene encoding endothiapepsin, *epn-1*. Based on Northern analysis, *lac-1* transcripts were previously reported to be down-regulated after hypovirus infection (8, 31, 41). CHV1-EP713 infection was reported to cause no change in endothiapepsin protein production and secretion (9). Based on microarray analysis, *lac-1* transcript levels remained unchanged and *epn-1* transcript levels decreased in EP155/CHV1-EP713 colonies, results confirmed by kinetic RT-PCR (data not shown). A major difference between the microarray study and the previ-

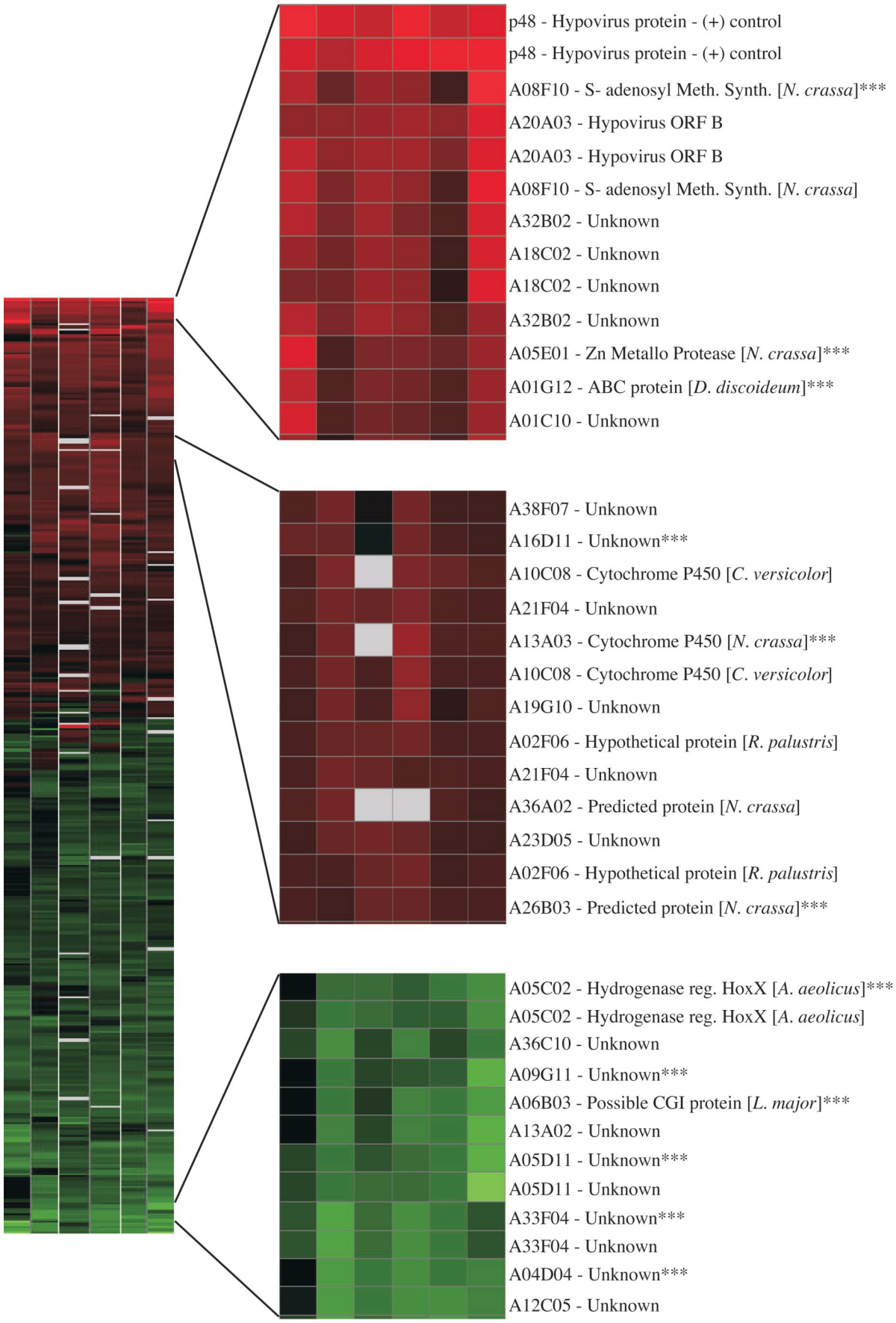

TABLE 3. Characteristics of selected differentially-expressed genes HoxX SAMS HSP70 GST SAHH

Fold change[a]	Clone	*E* value[b]	Description
10.56 (Down)	AEST-05-C-02	3.00*E*-27	HoxX (*Aquifex aeolicus*)
7.02 (Up)	AEST-08-F-10	5.00*E*-95	SAMS (*Neurospora crassa*)
2.76 (Up)	AEST-10-H-10	2.00*E*-77	HSP70 (*Ajellomyces capsulatus*)
9.84 (Up)	AEST-12-G-04	1.00*E*-38	GST (*Schizosaccharomyces pombe*)
5.07 (Up)	AEST-22-B-11	1.00*E*-105	SAHH (*Saccharomyces cerevisiae*)
3.02 (Down)	AEST-27-F-10	4.00*E*-31	Pro1 (*Neurospora crassa*)
2.77 (Down)	AEST-30-C-09	6.00*E*-65	Mst12 (*Magnaporthe grisea*)
ND	AEST-38-C-04	1.00*E*-108	HSP70 (*Neurospora crassa*)

[a] Average fold change up or down in EP155/CHV1-EP713 relative to EP155 as measured by real-time RT-PCR experiments (Table 2). ND, not determined.
[b] Strength of BLAST hit.

ous studies with *lac-1* and *epn-1* responses to CHV1-EP713 infection is that fungal mycelia were grown in liquid media in the previous studies and were grown on PDA-cellophane in the present study. In this regard, the *C. parasitica* microarray provides a powerful new tool with which to examine the influence of culture conditions on the magnitude and spectrum of hypovirus-induced symptom expression and host gene expression (37).

The microarray analysis presented here has expanded the number of identified *C. parasitica* genes that respond to hypovirus infection from less than 20 (13, 25) to nearly 300. It is clear from Table 1 that these genes are potentially associated with a wide range of biological processes. A comprehensive understanding of the significance of these cellular responses to hypovirus replication and hypovirus-mediated changes in host phenotype, including hypovirulence, will require additional studies. The 133 responsive genes of unknown function (supplemental data are available at http://www.umbi.umd.edu/~cbr/155_713SUPdata.pdf) represent an additional rich resource for future research. However, several host transcriptional responses that were identified and confirmed in this study merit discussion in terms of their potential relevance to hypovirus-mediated symptom expression and virus replication. Table 3 provides specific identities and associated BLAST information for all clones discussed below.

Hypovirus infection alters transcript accumulation for selected host stress response genes. The homologues of two genes that are transiently induced in classic responses to specific extracellular and intracellular stresses, heat shock protein 70 (HSP70) and glutathione *S*-transferase (GST), AEST-10-H-10 and AEST-12-G-04, respectively, are constitutively upregulated following CHV1-EP713 infection (35, 42). However, the increased accumulation of these transcripts was not accompanied by altered transcript accumulation for the many additional heat shock and classical stress response genes in the CEST library (12), suggesting the absence of a general stress response. Moreover, as indicated in Table 1, a second HSP70 homologue (AEST-38-C-04) showed reduced transcript accumulation. In this regard, the persistent nature of the hypovirus infection differs significantly from the acute changes associated with classical stress responses (16). While the increase in transcript accumulation for these putative stress response genes (Table 2) may be related to cellular defense responses to hypovirus infection, the absence of evidence for a general stress response raises the possibility that the HSP70 and GST homologues belong to a subset of genes induced by hypovirus infection to facilitate viral functions.

Although HSPs play a major role in protection against and recovery from thermal stress, several animal and plant viruses also have been shown to regulate HSP synthesis (1, 15, 21, 52). Recruitment of cellular HSP70s to facilitate virion assembly or genome replication has been demonstrated (11, 22, 49). Interestingly, plant closteroviruses actually encode an HSP70 that functions to facilitate cell-to-cell movement (38). It will be of considerable interest to examine whether disruption of the *C. parasitica* homologue (AEST-10-H-10) of HSP70 effects CHV1-EP713 replication.

GSTs belong to a superfamily of isoenzymes involved in the removal of reactive oxygen species and the conjugation of glutathione with various harmful ligands, including plant phenols and aflatoxins (46). Although fungal GSTs have not been extensively characterized, studies with other organisms have suggested that GSTs actually participate in a wide range of cellular functions not directly associated with detoxification (reviewed in reference 18). GST-mediated glutathione S thiolation of reactive cysteine residues has been implicated in regulating the activity of cellular proteins (27, 43), including kinases, transcription factors, and caspases, that function in apoptosis (17). In this regard, Kampranis et al. recently reported that a GST from tomato suppressed cell death caused by expression of the yeast inducer of apoptosis, Bax (24). In this context, viral induction of GST expression may represent a countermeasure to a cellular apoptosis-mediated defense response (48). It is also worth considering the possibility that increased glutathione S thiolation of cellular transcription factors contributes to virus-mediated changes in gene expression

FIG. 2. Hiearchical clustering of 295 differentially expressed clones (see Materials and Methods). Each clone is represented twice on the chip. Red squares indicate clones with increased transcript abundance and green squares indicate clones with decreased abundance after hypovirus infection. Gray blocks indicate missing data; black blocks indicate no differential gene expression. Each row represents six independent transcript abundance measurements for a specific clone. Each column represents a different hybrization experiment. Clones marked with asterisks were confirmed by real-time RT-PCR (Table 2). "A" in clone designations represents "AEST"; +, positive; Meth. Synth., methionine synthetase; Prot., protein; ABC, ATP-binding cassette; reg., regulation.

and symptom expression. The constitutive elevation of GST homologue transcript levels certainly warrants an examination of the effect of hypovirus infection on the cellular redox balance.

CHV1-EP713 infection substantially elevates transcript accumulation for homologues of SAMS and SAHH. Kawalleck et al. (6) previously reported the induction of *S*-adenosyl-L-methionine (SAMe) synthetase (SAMS) and S-adenosyl-L-homocysteine (SAH) hydrolase (SAHH) in plants following treatment with a fungal elicitor. This observation prompted the authors to suggest a link between plant defense responses and increased turnover of the activated methyl cycle. It was intriguing, therefore, to observe constitutive increases in transcript accumulation for homologues of SAMS (AEST-08-F-10) and SAHH (AEST-22-B-11) (Tables 2 and 3) of six- and fourfold, respectively, following CHV1-EP713 infection.

SAMS catalyzes the condensation of L-methionine and ATP to produce SAMe, which serves as the primary methyl donor in transmethylation reactions involving proteins, nucleic acids, fatty acids, and polysaccharides and as the precursor for polyamine synthesis. Transfer of the methyl group from SAMe results in the production of SAH. Since increased accumulation of SAH inhibits SAMe-dependent methylation, SAH is hydrolyzed by SAHH to L-homocysteine and adenosine. Given the central role of SAMe in cellular metabolism, the constitutive up-regulation of these key enzymes could be anticipated to have a number of possible metabolic or physiologic consequences. Altered transmethylation activity due to increased SAMe levels could influence physiologic processes ranging from protein synthesis to membrane integrity. Related alterations in polyamine biosynthesis could influence cell cycle progression and development in *C. parasitica*, as has been reported for the pathogenic fungus *Sclerotinia sclerotiorum* (39) and the fission yeast *Schizosaccharomyces pombe* (4). Associations between abnormal intracellular SAMe levels and altered rates of DNA mutations and genome stability due to changes in DNA methylation patterns have been suggested (28, 29, 30, 44), and SAHH has been reported to influence senescence and cell growth (33, 54) through its role in regulating homocysteine levels. In this context, persistent hypovirus infection of *C. parasitica* may provide a particulary useful model for examining the consequences of chronic RNA virus infection on the stability of host nuclear and organellar genomes.

Hypovirus infection alters a subset of *C. parasitica* transcriptional regulatory factors. There is increasing evidence to support the proposal that the pleiotrophic nature of hypovirus-mediated phenotypic changes is related to the perturbation of one or more key regulatory pathways (reviewed in reference 13). Thus, an understanding of the mechanisms underlying these changes is likely to require identification of key control points or elements, such as receptors, that are involved in initiating signaling pathways and transcription factors that convert signals into changes in gene expression. Therefore, it was of interest that only 3 of 26 genes classified under the molecular function category "transcription regulation/transcription factors" by Dawe et al. (12), AEST-27-F-10, AEST-30-C-09, and AEST-05-C-02, were found to be responsive to CHV1-EP713 infection; transcript accumulation was reduced by at least threefold for each gene (Table 2). Additionally, the products of two of the three genes are homologues of fungal transcription factors that have been reported to regulate processes that are altered by hypovirus infection. Transcription factor Pro1 (AEST-27-F-10) is involved in controlling fruiting body formation and sexual sporulation in several filamentous fungi (34). Mst12 (AEST-30-C-09) from the rice pathogen *Magnaporthe grisea*, a recently identified homologue of yeast Ste12, has been shown to be important in regulating infectious hypha growth (36). The third responsive regulatory factor homologue, HoxX (AEST-05-C-02), is part of a bacterial two-component system involved in the regulation of a hydrogenase that oxidizes hydrogen into constituent protons and electrons and passes the electrons to the electron transport chain (14). The potential significance of reduced expression of this putative regulatory factor to hypovirus infection is more difficult to envision. Significant on the basis of the absence of responsiveness were the *C. parasitica cpc1* cross-pathway control transcription factor (50) and a number of putative transcription factors, including homologues of transcription factor PacC from *N. crassa*, involved in regulation of the pH response, *N. crassa* Cys-3, involved in regulation of sulfur metabolism, the *hac1* transcription factor from *Hypocrea jecorinal*, and transcription factor CON7 from *M. grisea*.

In addition to revealing new hypotheses for testing, the *C. parasitica* microarray now provides the opportunity to address a number of long-standing questions about hypovirus infection. It will now be possible to examine whether hypoviruses that differ in the severity of symptom expression (6) elicit similar or quite different transcriptional responses by the host. Additionally, it should be possible to determine whether a symptom-inducing, hypovirus-encoded gene product, such as p29 (10, 47), alters the expression of a specific set of cellular genes. In combination with a collection of available *C. parasitica* signaling mutants, microarray analysis could be used to identify sets of cellular genes that are regulated through specific signaling pathways and simultaneously monitor the effects of hypovirus infection on their expression. It is anticipated that this information, in turn, will provide insight into the roles of specific cellular genes and signaling pathways in the elaboration of specific virus-mediated phenotypic changes, including attenuation of fungal virulence.

ACKNOWLEDGMENT

This work was supported in part by Public Health Service grant GM55981 to D. L. Nuss.

REFERENCES

1. **Aranda, M. A., M. Escaler, D. Wang, and A. J. Maule.** 1996. Induction of HSP70 and polyubiquitin expression associated with plant virus replication. Proc. Natl. Acad. Sci. USA **93:**15289–15293.
2. **Buck, K. W. (ed.).** 1986. Fungal virology—an overview, p. 2–84. CRC Press, Inc., Boca Raton, Fla.
3. **Bustin, S. A.** 2002. Quantification of mRNA using real-time reverse transcription PCR (RT-PCR): trends and problems. J. Mol. Endocrinol. **29:**23–39.
4. **Chattopadhyay, M. K., C. W. Tabor, and H. Tabor.** 2002. Absolute requirement of spermidine for growth and cell cycle progression of fission yeast (Schizosaccharomyces pombe). Proc. Natl. Acad. Sci. USA **93:**10330–10334.
5. **Chen, B., S. Gao, G. H. Choi, and D. L. Nuss.** 1996. Extensive alteration of fungal gene transcript accumulation and elevation of G-protein-regulated cAMP levels by a virulence-attenuating hypovirus. Proc. Natl. Acad. Sci. USA **93:**7996–8000.
6. **Chen, B., and D. L. Nuss.** 1999. Infectious cDNA clone of hypovirus CHV1-Euro7: a comparative virology approach to investigate virus-mediated hypovirulence of the chestnut blight fungus *Cryphonectria parasitica*. J. Virol. **73:**985–992.
7. **Choi, G. H., B. Chen, and D. L. Nuss.** 1995. Virus-mediated or transgenic suppression of a G-protein alpha subunit and attenuation of fungal virulence. Proc. Natl. Acad. Sci. USA **92:**305–309.

8. **Choi, G. H., T. G. Larson, and D. L. Nuss.** 1992. Molecular analysis of the laccase gene from the chestnut blight fungus and selective suppression of its expression in an isogenic hypovirulent strain. Mol. Plant-Microbe Interact. **5:**119–128.
9. **Choi, G. H., D. M. Pawlyk, B. Rae, R. Shapira, and D. L. Nuss.** 1993. Molecular analysis and overexpression of the gene encoding endothiapepsin, an aspartic protease from *Cryphonectria parasitica*. Gene **125:**135–141.
10. **Craven, M. G., D. M. Pawlyk, G. H. Choi, and D. L. Nuss.** 1993. Papain-like protease p29 as a symptom determinant encoded by a hypovirulence-associated virus of the chestnut blight fungus. J. Virol. **67:**6513–6521.
11. **Cripe, T. P., S. E. Delos, P. A. Estes, and R. L. Garcea.** 1995. In vivo and in vitro association of hsc70 with polyomavirus capsid proteins. J. Virol. **69:** 7807–7813.
12. **Dawe, A. L., V. C. McMains, M. Panglao, S. Kasahara, B. Chen, and D. L. Nuss.** 2003. An ordered collection of expressed sequences from *Cryphonectria parasitica* and evidence of genomic microsynteny with *Neurospora crassa* and *Magnaporthe grisea*. Microbiology **149:**2373–2384.
13. **Dawe, A. L., and D. L. Nuss.** 2001. Hypoviruses and chestnut blight: exploiting viruses to understand and modulate fungal pathogenesis. Annu. Rev. Genet. **35:**1–29.
14. **Durmowicz, M. C., and R. J. Maier.** 1997. Roles of HoxX and HoxA in biosynthesis of hydrogenase in *Bradyrhizobium japonicum*. J. Bacteriol. **179:** 3676–3682.
15. **Escaler, M., M. A. Aranda, C. L. Thomas, and A. J. Maule.** 2000. Pea embryonic tissues show common responses to the replication of a wide range of viruses. Virology **267:**318–325.
16. **Estruch, F.** 2000. Stress-controlled transcription factors, stress-induced genes and stress tolerance in budding yeast. FEMS Microbiol. Rev. **24:**469–486.
17. **Fernandez-Checa, J. C.** 2003. Redox regulation and signaling lipids in mitochondrial apoptosis. Biochem. Biophys. Res. Commun. **304:**471–479.
18. **Filomeni, G., G. Rotilio, and M. R. Ciriolo.** 2002. Cell signalling and the glutathione redox system. Biochem. Pharmacol. **64:**1057–1064.
19. **Galagan, J. E., S. E. Calvo, K. A. Borkovich, E. U. Selker, N. D. Read, D. Jaffe, W. FitzHugh, L. J. Ma, S. Smirnov, S. Purcell, B. Rehman, T. Elkins, et al.** 2003. The genome sequence of the filamentous fungus *Neurospora crassa*. Nature **422:**859–868.
20. **Gao, S., and D. L. Nuss.** 1996. Distinct roles for two G protein alpha subunits in fungal virulence, morphology, and reproduction revealed by targeted gene disruption. Proc. Natl. Acad. Sci. USA **93:**14122–14127.
21. **Glotzer, J. B., M. Saltik, S. Chiocca, A. I. Michou, P. Moseley, and M. Cotton.** 2000. Activation of heat-shock response by an adenovirus is essential for virus replication. Nature **407:**207–211.
22. **Holstein, S. E., H. Ungewickell, and E. Ungewickell.** 1996. Mechanism of clathrin basket dissociation: separate functions of protein domains of the DnaJ homologue auxilin. J. Cell Biol. **135:**925–937.
23. **Johnson, M. R., K. Wang, J. B. Smith, M. J. Heslin, and R. B. Diasio.** 2000. Quantitation of dihydropyrimidine dehydrogenase expression by real-time reverse transcription polymerase chain reaction. Anal. Biochem. **278:**175–184.
24. **Kampranis, S. C., R. Damianova, M. Atallah, G. Toby, G. Kondi, P. N. Tsichlis, and A. M. Makris.** 2000. A novel plant glutathione S-transferase/peroxidase suppresses Bax lethality in yeast. J. Biol. Chem. **275:**29207–29216.
25. **Kang, H.-S., J.-W. Choi, S.-M. Park, B. Cha, M.-S. Yang, and D.-H. Kim.** 2000. Ordered differential display from *Cryphonectria parasitica*. Plant Pathol. J. **16:**142–146.
26. **Kawalleck, P., G. Plesch, K. Hahlbrock, and I. E. Somssich.** 1992. Induction by fungal elicitor of S-adenosyl-L-methionine synthetase and S-adenosyl-L-homocysteine hydrolase mRNAs in cultured cells and leaves of *Petroselinum crispum*. Proc. Natl. Acad. Sci. USA **89:**4713–4717.
27. **Klatt, P., and S. Lamas.** 2000. Regulation of protein function by S-glutathiolation in response to oxidative and nitrosative stress. Eur. J. Biochem. **267:**4928–4944.
28. **Kricker, M. C., J. W. Drake, and M. Radman.** 1992. Duplication-targeted DNA methylation and mutagenesis in the evolution of eukaryotic chromosomes. Proc. Natl. Acad. Sci. USA **89:**1075–1079.
29. **Laird, P. W., L. Jackson-Grusby, A. Fazeli, S. L. Dickinson, W. E. Jung, E. Li, R. A. Weinberg, and R. Jaenisch.** 1995. Suppression of intestinal neoplasia by DNA hypomethylation. Cell **81:**197–205.
30. **Laird, P. W., and R. Jaenisch.** 1994. DNA methylation and cancer. Hum. Mol.Genet. (Spec.No.)**:**487–1495.
31. **Larson, T. G., G. H. Choi, and D. L. Nuss.** 1992. Regulatory pathways governing modulation of fungal gene expression by a virulence-attenuating mycovirus. EMBO J. **11:**4539–4548.
32. **Larson, T. G., and D. L. Nuss.** 1994. Altered transcriptional response to nutrient availability in hypovirus-infected chestnut blight fungus. EMBO J. **13:**5616–5623.
33. **Lo, S. C., L. Hamer, and J. E. Hamer.** 2002. Molecular characterization of a cystathionine beta-synthase gene, CBS1, in *Magnaporthe grisea*. Eukaryot. Cell **1:**311–314.
34. **Masloff, S., S. Jacobsen, S. Poggeler, and U. Kuck.** 2002. Functional analysis of the C6 zinc finger gene pro1 involved in fungal sexual development. Fungal Genet. Biol. **36:**107–116.
35. **Morimoto, R. I., A. Tissieres, and C. Georgopoulos (ed.).** 1994. The biology of heat shock proteins and molecular chaperones, p. 1–610. Cold Spring Harbor Laboratory Press, Cold Spring Harbor, N.Y.
36. **Park, G., C. Xue, L. Zheng, S. Lam, and J. R. Xu.** 2002. MST12 regulates infectious growth but not appressorium formation in the rice blast fungus *Magnaporthe grisea*. Mol. Plant-Microbe Interact. **15:**183–192.
37. **Parsley, T. B., B. Chen, L. M. Geletka, and D. L. Nuss.** 2002. Differential modulation of cellular signaling pathways by mild and severe hypovirus strains. Eukaryot. Cell **1:**401–413.
38. **Peremyslov, V. V., Y. Hagiwara, and V. V. Dolja.** 1999. HSP70 homolog functions in cell-to-cell movement of a plant virus. Proc. Natl. Acad. Sci. USA **96:**14771–14776.
39. **Pieckenstain, F. L., A. Garriz, E. M. Chornomaz, D. H. Sanchez, and O. A. Ruiz.** 2001. The effect of polyamine biosynthesis inhibition on growth and differentiation of the phytopathogenic fungus *Sclerotinia sclerotiorum*. Antonie Leeuwenhoek **80:**245–253.
40. **Quackenbush, J.** 2002. Microarray data normalization and transformation. Nat. Genet. **32**(Suppl.)**:**496–501.
41. **Rigling, D., U. Heiniger, and H. R. Hohl.** 1989. Reduction of laccase activity in dsRNA-containing hypovirulent strains of *Cryphonectria* (*Endothia*) *parasitica*. Phytopathology **79:**219–223.
42. **Salinas, A. E., and M. G. Wong.** 1999. Glutathione S-transferases—a review. Curr. Med. Chem. **6:**279–309.
43. **Schafer, F. Q., and G. R. Buettner.** 2001. Redox environment of the cell as viewed through the redox state of the glutathione disulfide/glutathione couple. Free Radic. Biol. Med. **30:**1191–1212.
44. **Selker, E. U.** 1990. DNA methylation and chromatin structure: a view from below. Trends Biochem. Sci. **15:**103–107.
45. **Shapira, R., G. H. Choi, and D. L. Nuss.** 1991. Virus-like genetic organization and expression strategy for a double-stranded RNA genetic element associated with biological control of chestnut blight. EMBO J. **10:**731–739.
46. **Sheehan, D., G. Meade, V. M. Foley, and C. A. Dowd.** 2001. Structure, function and evolution of glutathione transferases: implications for classification of non-mammalian members of an ancient enzyme superfamily. Biochem. J. **360:**1–16.
47. **Suzuki, N., and D. L. Nuss.** 2002. Contribution of protein p40 to hypovirus-mediated modulation of fungal host phenotype and viral RNA accumulation. J. Virol. **76:**7747–7759.
48. **Tschopp, J., M. Thome, K. Hofmann, and E. Meinl.** 1998. The fight of viruses against apoptosis. Curr. Opin. Genet. Dev. **8:**82–87.
49. **Ungewickell, E., H. Ungewickell, S. E. Holstein, R. Lindner, K. Prasad, W. Barouch, B. Martin, L. E. Greene, and E. Eisenberg.** 1995. Role of auxilin in uncoating clathrin-coated vesicles. Nature **378:**632–635.
50. **Wang, P., T. G. Larson, C. H. Chen, D. M. Pawlyk, J. A. Clark, and D. L. Nuss.** 1998. Cloning and characterization of a general amino acid control transcriptional activator from the chestnut blight fungus *Cryphonectria parasitica*. Fungal Genet. Biol. **23:**81–94.
51. **Wang, X., S. Ghosh, and S. W. Guo.** 2001. Quantitative quality control in microarray image processing and data acquisition. Nucleic Acids Res. **29:**E75.
52. **Whitham, S. A., S. Quan, H. S. Chang, B. Cooper, B. Estes, T. Zhu, X. Wang, and Y. M. Hou.** 2003. Diverse RNA viruses elicit the expression of common sets of genes in susceptible Arabidopsis thaliana plants. Plant J. **33:**271–283.
53. **Wu, T. D.** 2001. Analysing gene expression data from DNA microarrays to identify candidate genes. J. Pathol. **195:**53–65.
54. **Xu, D., R. Neville, and T. Finkel.** 2000. Homocysteine accelerates endothelial cell senescence. FEBS Lett. **470:**20–24.